AUTHOR(S): TOKODE, O., PRABHU, R., LAWTON, L.A. and ROBERTSON, P.K.J.

TITLE: The effect of pH on the photonic efficiency of the destruction of methyl orange under controlled periodic illumination with UV-LED sources.

YEAR: 2014

Publisher citation: TOKODE, O., PRABHU, R., LAWTON, L.A. and ROBERTSON, P.K.J. 2014. The effect of pH on the photonic efficiency of the destruction of methyl orange under controlled periodic illumination with UV-LED sources. Chemical engineering journal [online], 246, pages 337-342. Available from: http://dx.doi.org/10.1016/j.cej.2014.03.002

OpenAIR citation: TOKODE, O., PRABHU, R., LAWTON, L.A. and ROBERTSON, P.K.J. 2014. The effect of pH on the photonic efficiency of the destruction of methyl orange under controlled periodic illumination with UV-LED sources. Chemical engineering journal, 246, pages 337-342. Held on OpenAIR [online]. Available from: http://openair.rgu.ac.uk

The effect of pH on the photonic efficiency of the destruction of methyl orange under controlled periodic illumination with UV-LED sources

Oluwatosin Tokode, Radhakrishna Prabhu, Linda A Lawton and Peter K. J. Robertson.

IDeaS, Innovation, Design and Sustainability Research Institute, Robert Gordon University, Schoolhill, Aberdeen, AB10 1FR, UK.

Abstract

The nature of photon interaction and reaction pH can have significant impacts on semiconductor photocatalysis. This paper describes the effect of pH on the photonic efficiency of photocatalytic reactions in the aqueous phase using TiO_2 catalysts. The reactor was irradiated using periodic illumination with UV LEDS through control of the illumination duty cycle (γ) through a series of light and dark times (T_{on}/T_{off}). Photonic efficiencies for methyl orange degradation were found to be comparable at high γ irrespective of pH. At lower γ, pH effects on photonic efficiency were very distinct across acidic, neutral and alkaline pH indicating an effect of complementary parameters. The results suggest photonic efficiency is greatest as illumination time, T_{on} approaches interfacial electron-transfer characteristic time which is within the range of this study or charge-carrier lifetimes upon extrapolation and also when electrostatic attraction between surface-trapped holes, $\{Ti^{IV}OH^{\cdot}\}_{ads}^{+}$ and substrate molecules is strongest.

Keywords

TiO_2 Photocatalysis, pH effect, Methyl orange, Interfacial electron-transfer, Periodic illumination, UV-LED, Photonic efficiency

1. Introduction

The fundamental principles, mechanisms and applications of semiconductor photocatalysis using titanium dioxide (TiO_2) have been widely reported in the scientific literature [1-3]. The surface characteristics of TiO_2, redox reactions which take place on the surface and the role of charge-carriers and photogenerated intermediates (hydroxyl radical and superoxide) have also been investigated and well documented [4-7]. Photocatalytic oxidation is initiated when the semiconductor particle absorbs photons having energy (hv) equal to or greater than the bandgap of anatase (E_{bg} = 3.2 eV) [8]. Upon band gap excitation, electron and holes are photogenerated and for productive photocatalysis to occur, trapping of the photogenerated holes (h_{vb}^+) or electrons (e_{cb}^-) or both is necessary. This takes place on the surface of the photocatalyst, in traps located below the edge of the conduction band where they engage in oxidation and reduction of adsorbed molecules respectively [9,10]. The photogenerated h_{vb}^+ and e_{cb}^- are highly reactive with standard redox potentials of +2.53 and -0.52 respectively and can directly take part in the oxidation or reduction of substrates or indirectly through less reactive intermediates [11]. During photocatalytic reactions, the TiO_2 catalyst surface is covered by adsorbed O_2 and OH^- molecules which play significant roles in interfacial charge-transfer; O_2 is an efficient electron scavenger, while the adsorbed OH^- provide efficient hole traps [12]. Degussa (Evonik) P25 TiO_2 catalyst, which exhibits a high activity in photocatalytic reactions has been widely investigated as a photocatalyst and has been accepted as the de-facto standard in the research community [13].

The pH of the TiO_2 nanoparticle suspension plays an important role in photocatalytic reactions taking place on the TiO_2 surface. It can have significant influence on particle stability and/or aggregation, Fermi-level shifts which determine reduction potentials of electrons, band edge positions and electrostatic interactions of electron donors and acceptors [8,14]. The effect of pH on photocatalytic processes has been reported to influence the process in a number of ways including; a weak dependence of the reaction rate on pH [15], higher photocatalytic conversions at both acidic and alkaline pH, varying effects of pH in the presence of different cations, anions and neutral molecules [16], pH independent photooxidation rates [17] and the formation of intermediates [18]. The pH also has an influence on the efficiency of the photocatalytic process. Kormann et al. [16] first investigated the influence of pH on photocatalytic efficiency and reported that the photonic efficiency of TiO_2 catalysts at low pH can be decreased by simple anions such as HCO_3^- and Cl^- which have a negligible effect at high pH. Cornu et al. [19] found higher photocatalytic quantum yields at extreme pH as a result of a shift in the electrical potential of TiO_2 particles. As a result of these different effects, the interpretation of the effects of pH on photocatalytic processes can sometimes be problematic.

Studying the effects of pH under controlled periodic illumination (CPI) [20,21] can provide information on the pH-influenced dynamics of the redox reactions taking place during photocatalytic oxidation. In the CPI technique the photocatalytic reactor is irradiated using a series of alternate light and dark periods (T_{on}/T_{off}) which was previously reported as a means of increasing the photonic efficiency and conversion rates in TiO_2 photocatalysis [19-21]. Using this process, Cornu et al. [19] observed two distinct transitions in the differential reactivity of oxidizing and reducing species in methyl orange photooxidation. The characteristic times of these transitions was determined to be an exponential function of the solution pH. The pH can also have a strong influence on the standard driving force for interfacial charge transfer [22]. In alkaline media, the standard redox potential of e_{cb}^- is more negative while in acidic media results the potential of h_{vb}^+ can shift to more positive potentials [19]. CPI can be used to ensure T_{on} approaches charge-carrier lifetimes thus reducing carrier recombination or design T_{on} to match the characteristic time for interfacial electron-transfer to O_2 which is the slowest step in the photocatalytic reaction [2]. Likewise T_{off} which is facilitates the replenishment of O_2 can also be adjusted to an optimum duration to facilitate further removal of excess e_{cb}^- generated in the next T_{on} period[23].

In this study, the effect of pH on the photonic efficiency of TiO_2 photocatalysis has been investigated by studying the photodegradation of methyl orange within a range of γ under continuous and controlled periodic illumination. Methyl orange dye was selected for the study because of its anionic nature which corresponds to the electrostatic interactions required for the study and also because it absorbs UV light at a wavelength greater than the illumination source wavelength. Ultra-violet light emitting diodes (UV-LEDs), which have recently become an alternative UV source to conventional lamps in photocatalysis research [24-27] have the advantage of high efficiency, minimum heat generation, suitability for periodic illumination, narrow band emission and long life [28,29]. This paper establishes the use of UV-LEDs to study the effect of pH on photonic efficiency of TiO_2 photocatalysis under controlled periodic illumination. The triple effects of pH, γ and characteristic times of primary redox processes as well as the role of oxidizing species on the photonic efficiency trends in the photocatalytic reaction have also been investigated.

2. Experimental

2.1. Materials

Experiments were performed by irradiating TiO_2 suspensions in a stirred photoreactor, the TiO_2 catalyst (Degussa P25) was supplied by Evonik and used as received. Methyl orange dye supplied by Sigma-Aldrich was used as the model pollutant. A high loading of the TiO_2 photocatalyst at 5 g/L which was the optimum for the low UV intensity employed in the experimental setup (fig. 1.) was suspended in 100 mL methyl orange solution made in distilled water with concentration of $1x10^{-5}$ M. The pH values of the resulting suspension were adjusted using carbonate-bicarbonate buffer capsules for alkaline pH and nitric acid for acidic pH; both supplied by Sigma-Aldrich. An annular type slurry photoreactor made of Perspex was employed for the study; it consisted of an array of UV-LEDs in strips as the source of illumination and a magnetic stirrer for mixing. A detailed schematic diagram of this photoreactor is described in a previous study [20].

Figure 1.

2.2. Methods

The photocatalytic degradation of methyl orange solution was carried out over a period of 170 min including 30 min of dark adsorption. The dark adsorption period was experimentally determined as the time taken for adsorption equilibrium at room temperature. The pH adjustments only resulted in more dye molecules adsorbed with no impact on time taken for the dark adsorption equilibration. The TiO_2 suspension was illuminated under steady and intermittent UV light regimes resulting in five duty cycles, each with varying light and dark times (T_{on}/T_{off}) as shown in Table 1. The array of LEDs, stirring of slurry and small diameter of the reaction vessel ensured maximum interaction between photons and catalyst and the elimination of dead zones within the reactor. Light pulses for intermittent illumination were generated by an electronic astable multivibrator. By determining the ratio of the total energy of the LEDs to the energy of a single photon, the incident photon flux for the experiment was determined to be 4.85 × 10^{-8} einsteins L^{-1} s^{-1}.

Table 1.

Sample aliquots of 1 mL were withdrawn with a syringe (B-D plastiplak) at regular intervals in triplicate and filtered with a Whatman 0.45 µm filter to separate the suspended TiO_2 nanoparticles from the samples. The filtered samples were analysed using a Perkin Elmer Lambda950 UV-VIS spectrometer and the measure of photonic efficiency, ϕ was determined using the method described by Sakthivel et al. [30].

3. Results and Discussion

Methyl orange is an anionic azo dye which absorbs UV light at the highest peak of 468 nm [31]. This material has a photooxidation pathway consisting of demethylation and hydroxylation processes and is chemically stable under UV irradiation at acidic, neutral and alkaline pH [32]. The photooxidation process is initiated by the illumination of the TiO_2 suspension to generate charge-carriers; e_{cb}^- and h_{vb}^+(1). The photogenerated holes oxidize preadsorbed H_2O and OH^- to produce $OH^\bullet$ radical (2). The results of this study propose methyl orange photooxidation by free $OH^\bullet$ radicals and surface-trapped $\{Ti^{IV}OH^\cdot\}_{ads}^+$ acting as the oxidizing agents with respect to γ and the pH of the solution. Most organic compounds, however, can also be oxidized directly by h_{vb}^+ depending on the experimental conditions [33,34].

$$TiO_2 + h\nu \rightarrow e^-_{cb} + h^+_{vb} \qquad (1)$$

$$h^+_{vb} + OH^- \rightarrow OH^\bullet \qquad (2)$$

Experiments were carried out to investigate the influence of pH on the photonic efficiency of methyl orange photooxidation in acidic, neutral and alkaline media at various γ. An initial concentration of $1x10^{-5}$ M was used and the experiments were carried out at pH 4, 7 and 9.6 with γ within the range $\gamma = 0.07 - 1.00$. Methyl orange showed a steady rate of degradation at all experimental conditions because the reaction pathway involves unstable intermediates that are less reactive than methyl orange and present in low concentrations [32,35]. A 100 percent degradation of the dye was observed before the total reaction time elapsed for pH 4 and 7 at $\gamma = 0.73$ and $\gamma = 1$ respectively (fig. 2) while degradation at pH 9.6 was slower and lower with the highest percentage degradation of 88 percent recorded at $\gamma = 1$.

Figure 2.

The photonic efficiency of the photooxidation reaction increased with decreasing γ. The photonic efficiencies were comparable for the three pH values at $\gamma = 1$, 0.73 and 0.49. In order to ensure accuracy in the calculation for percentage degradation and photonic efficiency profiles of the reaction at the various pH, the reaction time was taken to be the time from the start of the reaction to a time just before complete degradation in pH 4 and 7 where the experiment continued for about 40 min after complete degradation. This was necessary to avoid inaccuracies in the calculation of the photonic efficiency which is expressed as the rate of reaction per incident photons therefore, a reaction time of 100 min was used for analysis of the results. The trend of methyl orange degradation and photonic efficiency remained the same after adjustment of data points indicating a fundamental trend in the reaction mechanism (fig 3).

Figure 3.

3.1. Effects of pH on photooxidation reaction

The experimental results showed a higher percentage of degradation as γ increased irrespective of pH and particularly at pH 4 and 7 which had almost twice the amount of degradation for pH 9.6 at each γ. This is due to the higher adsorption of methyl orange dye molecules onto the TiO_2 surface at acidic and neutral pH (fig. 4). Methyl orange is an anion with a negatively charged sulphonic group while TiO_2 (Degussa P25) has a point of zero charge of ~6.25 [36] and is positively charged in acidic media. This leads to a strong electrostatic attraction between the dye molecules and TiO_2 surface at these pH levels with the attraction at pH 4 stronger than that at pH 7. This pH influenced adsorption has been reported to be a critically important step for photocatalytic oxidation to take place and enhances photodegradation efficiency [37,38]. On the other hand in alkaline pH, TiO_2 is negatively charged giving rise to a coulombic repulsion between the negatively charged methyl orange substrate and TiO_2 surface [39] therefore, preventing or inhibiting the adsorption of substrate molecules on the catalyst hence resulting in a lower degradation of dye molecules.

Figure 4.

The degradation rates at pH 4 and pH 7 were observed to approach similar values. This could be as a result of pre-adsorption of the substrate on the catalyst surface prior to the start of the photocatalytic reaction. At pH 4, the electrostatic forces of attraction between surface-trapped hole/catalyst surface and dye molecules is strongest resulting in a high density of methyl orange ions on the surface without any catalyzed photoreaction which is characteristic of dyes taking place (3,4). This is due to the wavelength of UV illumination at 360 nm being lower than methyl orange UV absorption wavelength hence, limiting photon absorption by the catalyst.

$$\mathrm{Dye}_{ads} + h\nu \rightarrow \mathrm{Dye}^{*}_{ads} \qquad (3)$$

$$\mathrm{Dye}^{*}_{ads} + \mathrm{TiO_2} \rightarrow \mathrm{Dye}^{+\cdot}_{ads} + \mathrm{TiO_2}\,(e^-) \qquad (4)$$

At pH 7 the solution is neutral and electrostatic forces of attraction are weak however, the effects of pH on photocatalytic rates favour a faster degradation of methyl orange at this high pH because of a strong influence on the standard driving force for interfacial charge transfer [22]. It has been shown pH may affect the rates of TiO_2 photocatalysis by causing a shift in the electrochemical potential of the TiO_2 surface [40,41]. The standard redox potential of e_{cb}^- is more negative at high pH therefore facilitating O_2

reduction (5), which is the rate limiting step in photocatalytic reactions and consequently, a resulting in a higher level of methyl orange degradation at this pH. This effect was not observed at pH 9.6 most likely as a result of the very strong coulombic repulsion that exist between the TiO_2 surface and methyl orange molecules.

$$O_2 + e^-_{cb} \rightarrow TiO_2^- \qquad (5)$$

3.2. Role of active oxidative species

Photogenerated holes have a high quantum yield of 5.7×10^{-2} for ordinary photocatalytic reactions [42] and are readily trapped at the hydrated TiO_2 surface during the oxidation of surface-bound OH^- ion groups to $OH^\bullet$ radicals because of their small effective mass [43](6). Furthermore, $OH^\bullet$ radicals adsorbed on the surface of the hydroxylated TiO_2 particle are easily assimilated and are indistinguishable from surface-trapped holes [7]. The resulting $\{Ti^{IV}OH\cdot\}^+_{ads}$ is readily available for oxidative reactions with the surface adsorbed methyl orange (7).

$$h^+_{vb} + {>}Ti^{IV}OH \rightarrow \{Ti^{IV}OH\cdot\}^+ \qquad (6)$$

$$\{Ti^{IV}OH\cdot\}^+_{ads} + MO_{ads} \rightarrow \text{colourless product} \qquad (7)$$

Our results suggest that the two oxidizing species responsible for methyl orange photooxidation; surface-trapped holes $\{Ti^{IV}OH\cdot\}^+_{ads}$ and free $OH^\bullet$ radical are dominant at different pH when impacted on by a T_{on}/T_{off} cycle (fig 5.). Studies by Ishibashi et al. [42] have shown that quantum yields of $OH^\bullet$ radical production during TiO_2 photocatalysis are generally lower than those of h^+_{vb} . At high γ such that $\gamma \geq 0.49$, however, charge-carrier recombination occurs by second-order kinetics [44]. This means rapid depletion of charge-carriers especially the highly oxidative h_{vb}^+ before and after trapping. This leads to photooxidation in the bulk solution by free $OH^\bullet$

radical, the oxidative species with a lower redox potential being the predominant.

At pH < 7 with $\gamma \leq 0.49$, the reaction is characterised by low charge-carrier recombination because of the brief illumination periods and methyl orange molecule which acts as a hole scavenger being strongly bound to the photocatalyst surface due to the strong electrostatic attraction between the opposite charges. This leads to surface-mediated reactions being the predominating[45,46].

Figure 5.

At pH > 7 with $\gamma \geq 0.49$, the reaction is characterized by weak adsorption as a result of the coulombic repulsion between TiO_2, which has a negative charge in alkaline pH and the similarly charged dye anion. High charge-carrier recombination may also limit $\{Ti^{IV}OH\cdot\}^{+}{}_{ads}$ at the surface thus, the predominant oxidizing species is the free electrically neutral $OH^{\bullet}$ radical having an unpaired electron. The $OH^{\bullet}$ radical primarily attacks the unsaturated bonds on methyl orange molecule resulting in photooxidation of methyl orange by $OH^{\bullet}$ radical in the bulk solution [47](8).

$$OH\cdot_{bulk} + MO_{bulk} \rightarrow \text{colourless product} \qquad (8)$$

3.3. Overall effect pH and γ on photonic efficiency

The pH and γ both affect the dynamics of the photocatalytic reaction in separate ways, however, there is a combined effect of pH and γ on the photonic efficiency of the photocatalytic reaction. In figure 3, the photonic efficiency of methyl orange photodegradation follows a similar trend across the three pH values investigated when γ falls within the range $\gamma > 0.24$. In this region, the pH has a smaller influence on the photonic efficiency than

γ and the increasing efficiency observed is as a result of a decrease in the illumination time and a corresponding decrease in γ. Charge-carrier generation which occurs in $\sim10^{-15}$ [2] is typically high because of the prolonged T_{on} which far exceeds 10^{-15} and this leads to high recombination rates leading to low photonic efficiency. At $\gamma \leq 0.24$, the photonic efficiency of the reaction shows a peculiar trend as the effects of pH become significant and the divergence of the trend with respect to pH is emphasized with a further reduction in γ. At $\gamma = 0.07$, charge-carrier recombination is low and photonic efficiency reaches the highest value for all three pHs because of the decreasing γ and brief T_{on}. The photonic efficiency at this γ is found to be a function of pH and the observed increase is not the same across the pH values investigated.

The photonic efficiency at $\gamma = 0.07$ was greatest at pH 4 and lowest at pH 9.6 because of the resultant effect the pH, γ and oxidizing species all have on the photocatalytic reaction. The pH has a direct effect on the rate of interfacial-electron transfer which reduces with reducing pH [48] while γ is a function of T_{on} which inhibits charge-carrier recombination as T_{on} decreases [49,50]. Both parameters have an influence on the role of the oxidatising species in the reaction and also on optimizing the process of interfacial charge-transfer and charge-carrier lifetime for maximum photonic efficiency. The trend indicates that photonic efficiency is greatest when electrostatic attraction is highest at pH 4 with surface $\{Ti^{IV}OH\cdot\}^{+}{}_{ads}$ mediated oxidation and T_{on} approaches the characteristic time for interfacial-electron transfer which is in the millisecond domain, this trend can also be extrapolated to charge-carrier lifetimes which have characteristic times below the shortest T_{on} in this study.

4. Conclusion

Under controlled periodic illumination of TiO_2, photonic efficiency of photocatalytic oxidation in the aqueous phase is not only dependent on γ of illumination but the pH of the media. This study has investigated the resultant effect of pH and γ on methyl orange photodegradation and the results show little influence of pH at high γ. At low γ, the pH has a significant effect on photonic efficiency with the oxidative species and a match between T_{on} and interfacial electron-transfer also contributing to photonic efficiency enhancements. Data points at lower γ values were not achievable with the current illumination source, however, further work is ongoing at microsecond T_{on}/T_{off} cycles.

Acknowledgements.

The authors would like to thank the Scottish Funding Council who funded R. Prabhu's lectureship through the Northern Research Partnership's research pooling initiative in engineering.

References

1. D. Bahnemann, D. Bockelmann, R. Goslich, Mechanistic studies of water detoxification in illuminated TiO2 suspensions, Solar Energy Materials 24 (1991) 564-583.
2. M.R. Hoffmann , S.T. Martin , W. Choi , D.W. Bahnemann, Environmental Applications of Semiconductor Photocatalysis, Chem. Rev. 95 (1995) 69-96.
3. A. Mills, S. Le Hunte, An overview of semiconductor photocatalysis, J. Photochem. Photobiol. A. 108 (1997) 1-35.
4. D.W. Bahnemann, M. R. Hilgendorff , R. Memming, Charge Carrier Dynamics at TiO2 Particles Reactivity of Free and Trapped Holes, J. Phys. Chem. B 101 (1997) 4265–4275.
5. J.M Coronado, J.A. Maira, J.C. Conesa, K.L. Yeung, V. Augugliaro, J. Soria, EPR Study of the Surface Characteristics of Nanostructured TiO2 under UV Irradiation, Langmuir 17 (2001) 5368–5374.
6. U. Diebold, The surface science of titanium dioxide, Surface Science Reports 48 (2003) 53-229.
7. D. Lawless , N. Serpone , D. Meisel, Role of hydroxyl radicals and trapped holes in photocatalysis. A pulse radiolysis study, J. Phys. Chem. 95 (1991) 5166–5170.
8. L.A. Linsebigler , G. Lu , T.J. Yates, Photocatalytic on TiO2 Surfaces: Principles, Mechanisms, and selected results , Chem. Rev. 95 (1995) 735-758.
9. S.H. Szczepankiewicz, J.A. Moss, M. Hoffmann R., Slow Surface Charge Trapping Kinetics on Irradiated TiO2, J Phys Chem B 106 (2002) 2922-2927.
10. H. Wang, J. He, G. Gerrit Boschloo, H. Lindstrom, A. Hagfeldt, S. Lindquist, Electrochemical Investigation of Traps in a Nanostructured TiO2 Film, J Phys Chem B 105 (2001) 2529-2533.
11. A. Fujishima, T.N. Rao, D.A. Tryk, Titanium dioxide photocatalysis, Journal of Photochemistry and Photobiology C: Photochemistry Reviews 1 (2000) 1-21.
12. S.A. Bilmes, P. Mandelbaum, F. Alvarez, N.M Victoria, Surface and electronic structure of titanium dioxide photocatalysts, J. Phy. Chem. B, 104 (2000), 9851-9858.
13. B. Ohtani, O.O. Prieto-Mahaney, D. Li, R. Abe, What is Degussa (Evonik) P25? Crystalline composition analysis, reconstruction from isolated pure particles and photocatalytic activity test. Journal of Photochemistry and Photobiology A: Chemistry, 216 (2010), 179-182.
14. B. Siffert, J. Metzger, Study of the interaction of titanium dioxide with cellulose fibers in an aqueous medium, Colloids and Surfaces 53 (1991) 79-99.
15. A.M. Fox , T.M. Dulay, Heterogeneous photocatalysis, Chem. Rev. 93 (1993) 341-357.

16. C. Kormann, D.W. Bahnemann, M.R. Hoffmann, Photolysis of Chloroform and Other Organic Molecules in Aqueous TiO, Suspensions, Environ. Sci. Technol. 25 (1991) 494-500.
17. S. Kumar, A.P. Davis, Heterogeneous Photocatalytic Oxidation of Nitrotoluenes, Water Environ. Res. 69 (1997) 1238-1245.
18. W. Choi , M. Hoffmann R., Photoreductive Mechanism of CCl4 Degradation on TiO2 Particles and Effects of Electron Donors, Environ. Sci. Technol. 29 (1995) 1646–1654.
19. C.J.G. Cornu, A.J. Colussi, M.R. Hoffmann, Time Scales and pH Dependences of the Redox Processes Determining the Photocatalytic Efficiency of TiO2 Nanoparticles from Periodic Illumination Experiments in the Stochastic Regime, The Journal of Physical Chemistry B 107 (2003) 3156-3160.
20. O.I. Tokode, R. Prabhu, L.A. Lawton, P.K.J. Robertson, Effect of controlled periodic-based illumination on the photonic efficiency of photocatalytic degradation of methyl orange, Journal of Catalysis 290 (2012) 138-142.
21. J.G. Sczechowski, C.A. Koval, R.D. Noble, Evidence of critical illumination and dark recovery times for increasing the photoefficiency of aqueous heterogeneous photocatalysis, J. Photochem. Photobiol. A. 74 (1993) 273-278.
22. N.S. Lewis, Chemical control of charge transfer and recombination at semiconductor photoelectrode surfaces, Inorg. Chem. 44 (2005) 6900-6911.
23. G. Stewart , A.M. Fox , The Effect of Dark Recovery Time on the Photoefficiency of Heterogeneous Photocatalysis by TiO2 Suspended in Non-Aqueous Media, Res. Chem. Interm. 21 (1995) 933-938(6).
24. A. Jamali, R. Vanraes, P. Hanselaer, T. Van Gerven, A batch LED reactor for the photocatalytic degradation of phenol, Chemical Engineering and Processing: Process Intensification. http://dx.doi.org/10.1016/j.cep.2013.03.010
25. W. Hou, Y. Ku, Photocatalytic decomposition of gaseous isopropanol in a tubular optical fiber reactor under periodic UV-LED illumination, Journal of Molecular Catalysis A: Chemical 374–375 (2013) 7-11.
26. A.L.B. Baccaro, I.G.R. Gutz, Novel photoelectrocatalytic approach aiming at the digestion of water samples, estimation of organic matter content and stripping analysis of metals in a special UV-LED irradiated cell with a TiO2-modified gold electrode, Electrochemistry Communications 31 (2013) 28-30.
27. Z. Wang, J. Liu, Y. Dai, W. Dong, S. Zhang, J. Chen, CFD modeling of a UV-LED photocatalytic odor abatement process in a continuous reactor, J. Hazard. Mater. 215–216 (2012) 25-31.
28. S. Venkataramani, K.M. Davitt, H. Xu, J. Zhang, Y. Song, B.W. Connors, A.V. Nurmikko, Semiconductor ultra-violet light-emitting diodes for flash photolysis, J. Neurosci. Methods 160 (2007) 5-9.

29. T.S. Natarajan, K. Natarajan, C.H. Bajaj, J.R. Tayade, Energy Efficient UV-LED Source and TiO2 Nanotube Array-Based Reactor for Photocatalytic Application, Ind. Eng. Chem. Res. 50 (2011) 7753-7762.
30. S. Sakthivel, M.V. Shankar, M. Palanichamy, B. Arabindoo, D.W. Bahnemann, V. Murugesan, Enhancement of photocatalytic activity by metal deposition: characterisation and photonic efficiency of Pt, Au and Pd deposited on TiO2 catalyst, Water Res. 38 (2004) 3001-3008.
31. P. He, L. Wang, J. Xue, Z. Cao, Electrolytic treatment of methyl orange in aqueous solution using three-dimensional electrode reactor coupling ultrasonics, Environmental Technology 31 (2010) 417-422.
32. A.B. Prevot, A. Basso, C.Baiocchi, M. Pazzi, G. Marci, V. Augugliaro, L. Palmisano, E. Pramauro, Analytical control of photocatalytic treatments: degradation of a sulfonated azo dye. Analytical and bioanalytical chemistry, 378(2004), 214-220.
33. E.R. Carraway , A.J. Hoffman , M.R. Hoffmann, Photocatalytic Oxidation of Organic Acids on Quantum-Sized Semiconductor Colloids, Environ. Sci. Technol. 28 (1994) 786–793.
34. Y. Mao , C. Schoeneich , K.D. Asmus, Identification of organic acids and other intermediates in oxidative degradation of chlorinated ethanes on titania surfaces en route to mineralization: a combined photocatalytic and radiation chemical study, J. Phys. Chem. 95 (1991) 10080–10089.
35. M. Ge, C. Guo, X. Zhu, L. Ma, Z. Han, W. Hu, Y. Wang, Photocatalytic degradation of methyl orange using ZnO/TiO2 composites. Frontiers of Environmental Science & Engineering in China, 3 (2009), 271-280.
36. D. W. Bahnemann, M. Muneer, M. Haque, Titanium dioxide-mediated photocatalysed degradation of few selected organic pollutants in aqueous suspensions, Catalysis Today 124 (2007) 133-148.
37. K. Gude, V.M. Gun’ko, J.P. Blitz, Adsorption and photocatalytic decomposition of methylene blue on surface modified silica and silica-titania, Colloids Surf. Physicochem. Eng. Aspects 325 (2008) 17-20.
38. U.G. Akpan, B.H. Hameed, Parameters affecting the photocatalytic degradation of dyes using TiO2-based photocatalysts: A review, J. Hazard. Mater. 170 (2009) 520-529.
39. S.X. Li, S.J. Cai, F.Y. Zheng, Self assembled TiO2 with 5-sulfosalicylic acid for improvement its surface properties and photodegradation activity of dye. Dyes and Pigments, 95 (2012), 188-193.
40. M. Gratzel, Heterogeneous Photochemical Electron Transfer, CRC Press, Boca Raton, FL, 1989.
41. C.A. Brett, A.M. Oliveira-Brett, Electrochemistry: Principles, Methods and Applications, Oxford University Press, London, 1993.
42. K. Ishibashi, A. Fujishima, T. Watanabe, K. Hashimoto, Quantum yields of active oxidative species formed on TiO2 photocatalyst, J. Photochem. Photobiol. A. 134 (2000) 139-142.

43. S.H. Szczepankiewicz, J.A. Moss, M.R. Hoffmann, Electron Traps and the Stark Effect on Hydroxylated Titania Photocatalysts, J Phys Chem B 106 (2002) 7654–7658.
44. N. Serpone , D. Lawless , R. Khairutdinov, Subnanosecond Relaxation Dynamics in TiO2 Colloidal Sols (Particle Sizes Rp = 1.0-13.4 nm. Relevance to Heterogeneous Photocatalysis, J. Phys. Chem. 99 (1995) 16655-16661.
45. S. Tunesi, M. Anderson, Influence of chemisorption on the photodecomposition of salicylic acid and related compounds using suspended titania ceramic membranes, J. Phys. Chem. 95 (1991) 3399-3405.
46. W.Z. Tang, C.P. Huang, Photocatalyzed oxidation pathways of 2,4-dichlorophenol by CdS in basic and acidic aqueous solutions, Water Res. 29 (1995) 745-756.
47. N.J. Herak , W. Gordy, Interaction of hydrogen atoms and hydroxyl radicals with 5-halogen uracils, Proc. Natl. Acad. Sci. USA. 56 (1966) 1354–1360.
48. J. Moser, S. Punchihewa, P.P. Infelta, M. Graetzel, Surface complexation of colloidal semiconductors strongly enhances interfacial electron-transfer rates. Langmuir, 7 (1991), 3012-3018.
49. S. Upadhya , F.D. Ollis, Simple Photocatalysis Model for Photoefficiency Enhancement via Controlled, Periodic Illumination, J. Phys. Chem. B 101 (1997) 2625-2631.
50. H.W. Chen, Y. Ku, A. Irawan, Photodecomposition of *o*-cresol by UV-LED/TiO_2 process with controlled periodic illumination. Chemosphere, 69 (2007), 184-190.

Captions for Tables

Table 1: Light regimes for continuous and periodic illumination showing duty cycle and frequency of pulsing.

DUTY CYCLE (γ)	**Average UV Intensity ($\mu W/cm^2$)**	**T_{ON} (ms)**	**T_{OFF} (ms)**	**PERIOD (ms)**
0.07	12.5	72	904	976
0.24	42.7	234	740	974
0.49	87.2	474	500	974
0.73	129.9	708	266	974
1.00	178.0	CONTINUOUS ILLUMINATION		

Table 1.

Captions for Figures

Figure 1: Optimum loading for methyl orange photodegradation using the experimental setup.

Figure 2: (a) Amount of methyl orange photodegradation after total reaction time at acidic, neutral and alkaline pH; (b) photonic efficiency of methyl orange degradation at $\gamma = 0.07 - 1.00$.

Figure 3: Adjusted profiles at various duty cycles of (a) photodegradation of methyl orange; (b) photonic efficiency of methyl orange photodegradation.

Figure 4: Effect of pH on adsorption of methyl orange on TiO_2 surface.

Figure 5: Effect of pH and γ on the role of oxidizing species.

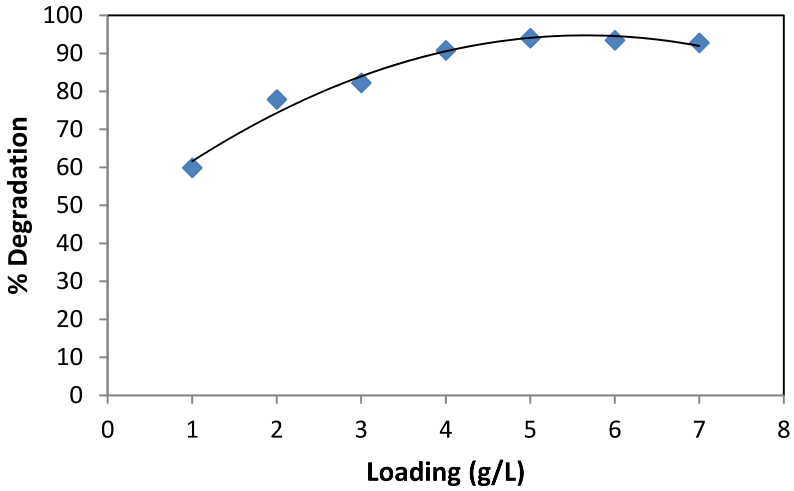
% Degradation
100
90
80
70
60
50
40
30
20
10
0
0
1
2
3
4
5
6
7
8
Loading (g/L)

Fig. 1.

(a)

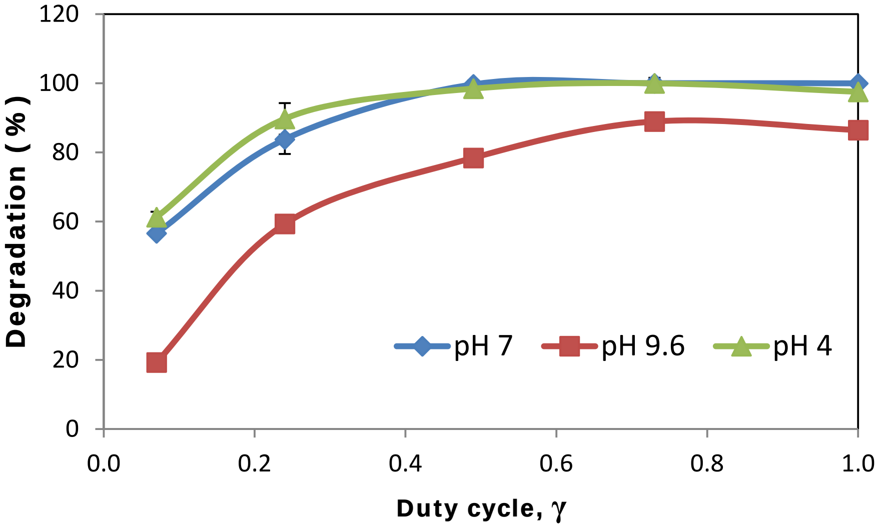
Degradation (%)
120
100
80
60
40
20
0
0.0
0.2
0.4
0.6
0.8
1.0
Duty cycle, γ
pH 7
pH 9.6
pH 4

(b)

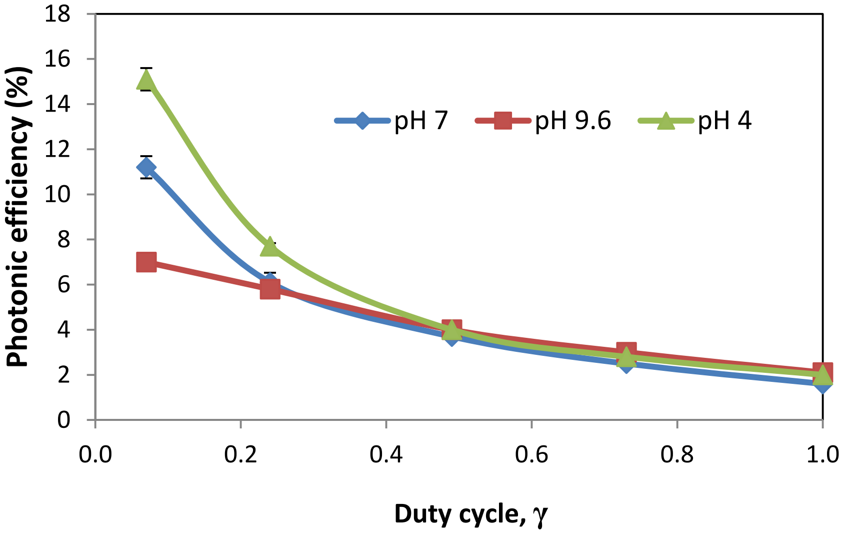
Photonic efficiency (%)
18
16
14
12
10
8
6
4
2
0
pH 7
pH 9.6
pH 4
0.0
0.2
0.4
0.6
0.8
1.0
Duty cycle, γ

Fig. 2.

(a)

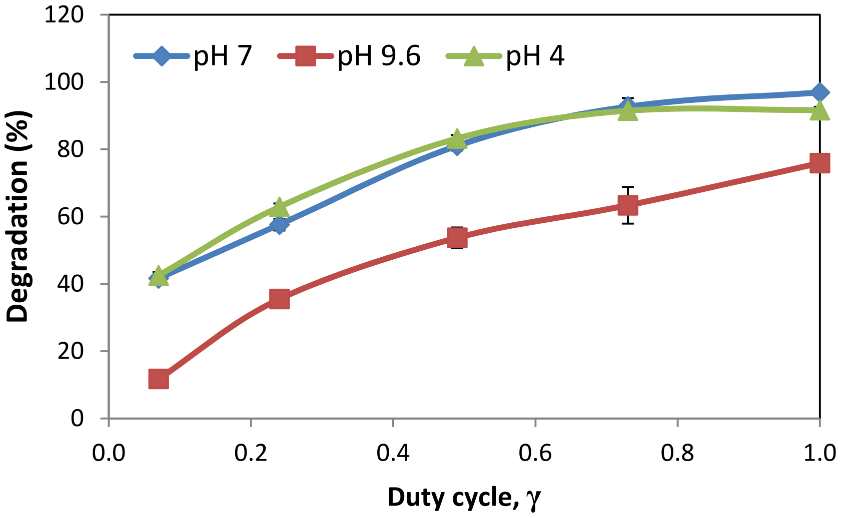
Degradation (%)
120
100
80
60
40
20
0
pH 7
pH 9.6
pH 4
0.0
0.2
0.4
0.6
0.8
1.0
Duty cycle, γ

(b)

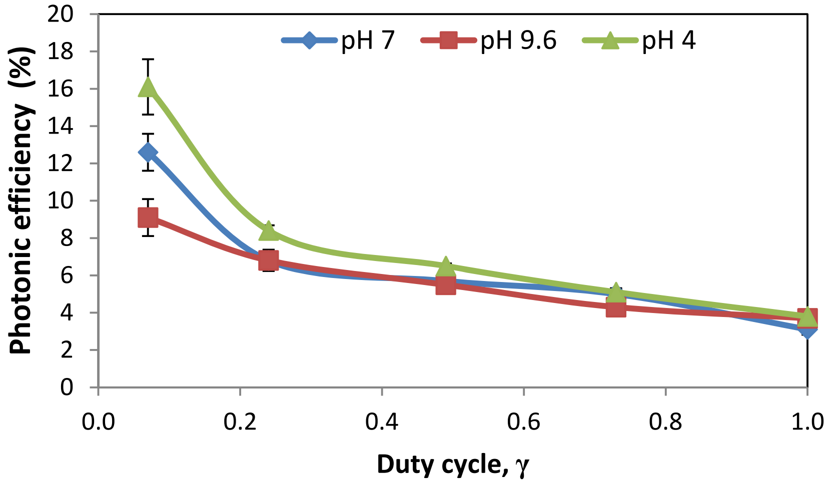
pH 7
pH 9.6
pH 4
Photonic efficiency (%)
20
18
16
14
12
10
8
6
4
2
0
0.0
0.2
0.4
0.6
0.8
1.0
Duty cycle, γ

Fig. 3.

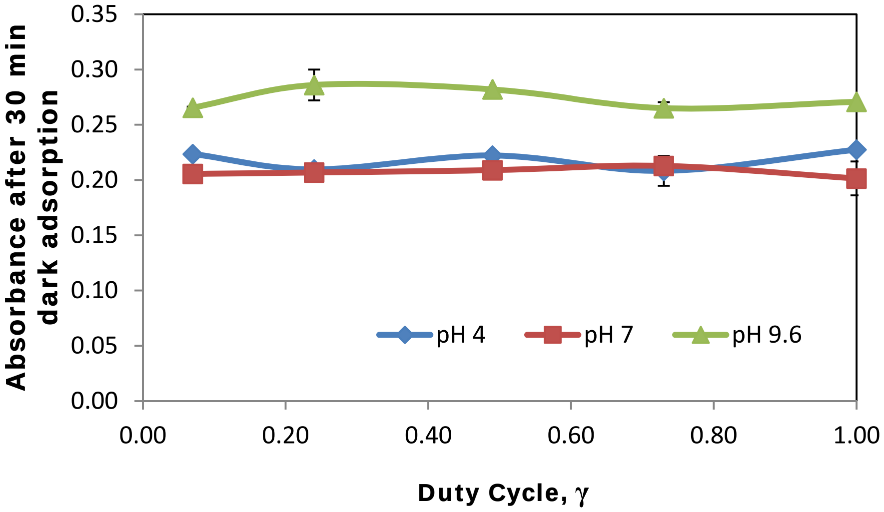
Absorbance after 30 min dark adsorption
0.35
0.30
0.25
0.20
0.15
0.10
0.05
0.00
pH 4
pH 7
pH 9.6
0.00
0.20
0.40
0.60
0.80
1.00
Duty Cycle, γ

Fig. 4.

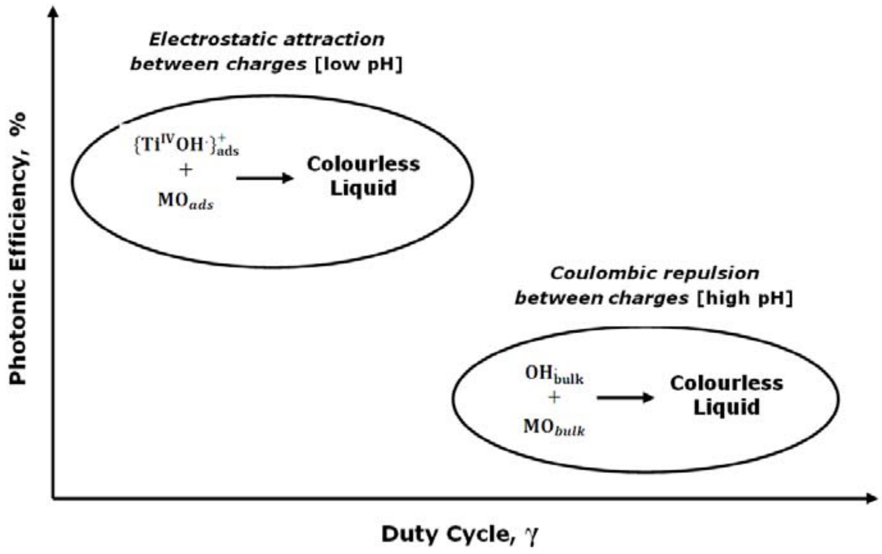
Electrostatic attraction between charges [low pH]
{Ti^IV OH·}+ads + MOads → Colourless Liquid
Coulombic repulsion between charges [high pH]
OH·bulk + MObulk → Colourless Liquid
Photonic Efficiency, %
Duty Cycle, γ

Fig. 5.